Analysis of Fractal Behaviour of Earthquakes in the Indian Subcontinent

A Dissertation

submitted in partial fulfillment of the
requirements for the awards of the degree of

Integrated Master of Technology
In
Geophysical Technology

Submitted by
Saurav Goyal

Under the guidance of
Dr Kamal

Department of Earth Sciences
Indian Institute of Technology, Roorkee
Roorkee-247667

May 16, 2019

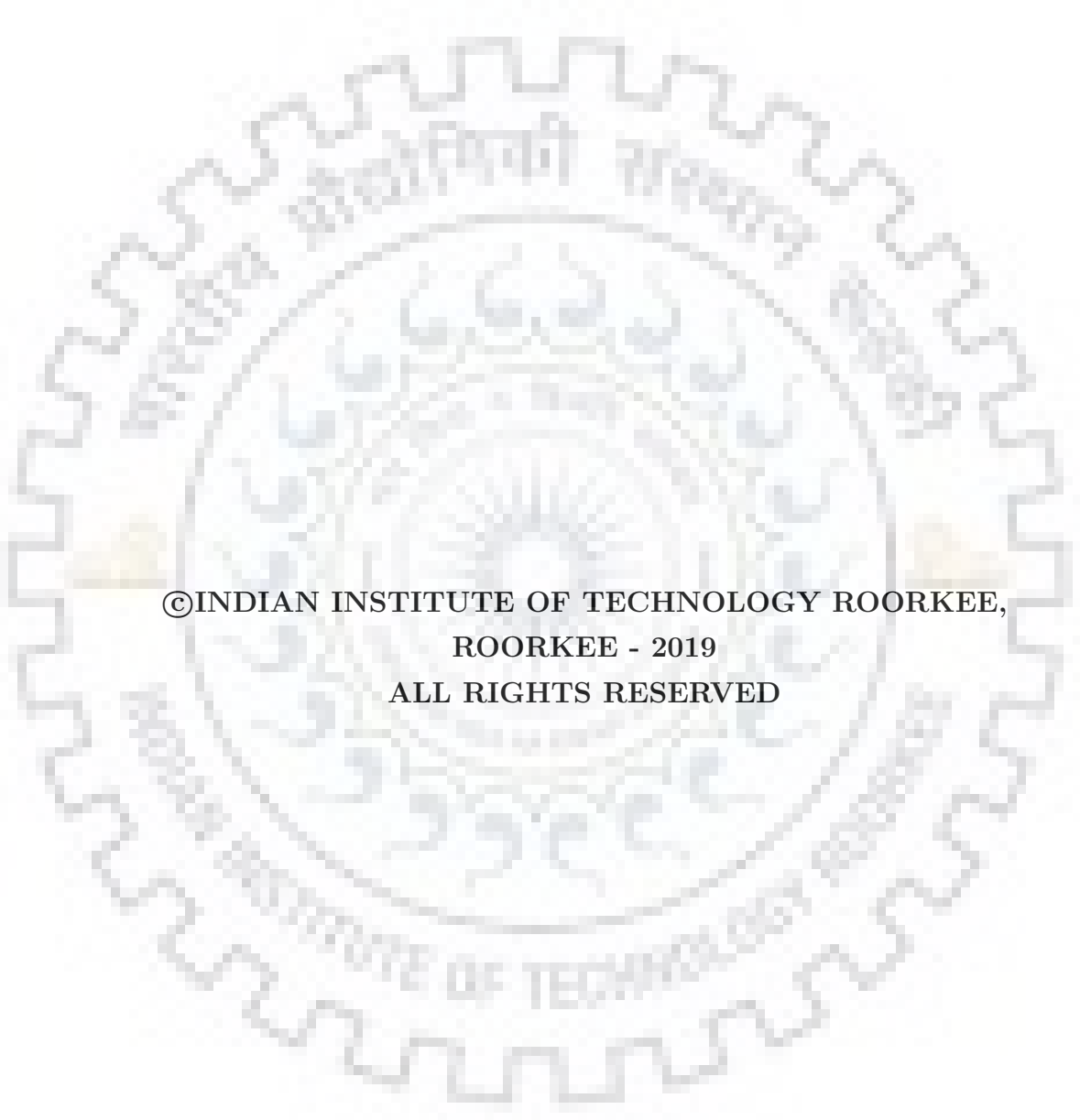

Declaration

I hereby declare that the work which is being presented in the thesis entitled **"Analysis of Fractal Behaviour of Earthquakes in the Indian Subcontinent"** in the partial fulfillment of the requirement for the award of the degree of *Integrated Master of Technology* in *Geophysical Technology* and submitted to the *Department of Earth Sciences, Indian Institute of Technology Roorkee*, is an authentic record of my own work carried out during a period from July 2018 to April 2019 under the supervision of **Dr Kamal, Associate Professor, Department of Earth Sciences, Indian Institute of Technology Roorkee**.

The matter presented in this report has not been submitted by me for the award of any other degree of this or any other institute.

I fully understand the implications of plagiarism and that if at any stage the above statement made by me is found to be incorrect; I shall be fully responsible for my act(s).

Saurav Goyal, 14411027
I.M.T. Geophysical Technology
Department of Earth Sciences
IIT Roorkee

Date: 16 March 2019
Place: Roorkee

CERTIFICATE

This is certified that the above statement made by the candidate is correct to the best of my knowledge.

Dr Kamal
Associate Professor
Department of Earth Sciences
IIT Roorkee

Date: 16 March 2019
Place: Roorkee

Abstract

The aim of this dissertation is to analyze and find a correlation, if any, between the earthquakes occurring in the Indian subcontinent. For two different sets of studies, the earthquakes occurring in the Himalayan and the Andaman-Sumatra region are mainly divided into four and six zones based on their tectonic similarity. The earthquake data of past 49 years (till 31-Dec-2018) was utilised for the purpose of this study.

When arranged chronologically, the seismic events produced a one dimensional time array of *coarse-grain magnitude* in accordance with the specific zone of their occurrence.

The coarse grain magnitudes are then read as 1, 4, and 6 bit fractal addresses for areas divided into 4 zones, and as one-bit fractal addresses for areas divided into 6 zones, using a MATLAB code. The images thus produced are analyzed to find correlation, if any, between the seismic zones. The images produced by assigning probabilities of occurrence of a seismic event in each zone, calculated using historical data and assuming all events are independent, reflects dissimilarity to the images produced by the actual earthquakes.

The results strengthens the idea that all the seismic events are not independent and there must exist a correlation between them. Now, the conclusion is based on the historical data in the given study area, and we can only determine the probability of occurrence of an event with respect to a given seismic activity by comparing the zone wise earthquake mapping and the pattern generated by assigning probabilities to each zone.

Acknowledgments

This dissertation would not have been possible without the proper guidance and support of Dr Kamal, Associate Professor, Department of Earth Sciences, IIT Roorkee. I thank him for mentoring me and guiding me through all the obstacles. His constant constructive criticism has helped me to refine my work and develop the skills that I have today.

I would also like to extend my thanks to my batch-mates and friends for their guidance and encouragement throughout my dissertation work. Special thanks to my friend Cyril Cyriac without whom this work would not have been possible.

I acknowledge the love and support of my family, who always stood by my side and all the people in Department of Earth Sciences, IIT Roorkee for their administrative support.

Date: 16 March 2019
Place: Roorkee

Saurav Goyal, 14411027
I.M.T. Geophysical Technology
Department of Earth Sciences
IIT Roorkee

Contents

List of Figures

Chapter 1

Introduction

Earthquakes are the sudden movements of the upper most layer of the Earth surface, caused due to rapid release of energy stored inside the rocks at or below the Earth's surface as a result of the stresses building up in the ever moving lithospheric plates in the Earth's crust.

Compressional stresses occur when rocks are pushed together i.e. they are pressed into one another. *Tensional stresses* occur when rocks are pulled apart i.e. they are being stretched farther than they would be otherwise. *Shear stresses* occur when rocks slide past each other in opposite directions, resulting in a lot of friction.

The energy released during such events radiates outward in all directions, and shakes the ground as it moves toward the surface. Depending upon the amount of energy released, the magnitude of shaking can either be so small that it can not be felt even by a human body, or it can be so huge that it can cause permanent damage to man-made structures and lead to the loss of life and property. The ground movements can be recorded in the form of the strength and the speed of the energy from the *hypocenter* of the breaking point using a *seismograph*.

Earthquakes (also called a quake, tremor, or temblor), are usually caused due to ruptures in the Earth's (sub)surface as a result of the stress build up, but can also be attributed to other - either man-made or natural - factors such as volcanic activity, landslides, nuclear tests, mine blasts etcetra. The global earthquake distribution is predominately concentrated along the boundaries of the tectonic plates, with a vast a majority of them located near the convergent plate bound-

aries (subduction and collision) than the divergent plate boundaries (rift valleys and mid-ocean ridges). But not all earthquakes occur near plate boundaries. Some, for example - the Killari earthquake in India in 1993 or the immensely destructive Lisbon earthquake of 1755, occurred within stable cratonic areas.

Earthquakes are known to be potential of causing mass destruction. An earthquake of sufficient energy located beneath the seabed can even cause a *tsunami*. Hence, it is of prime importance that we are able to predict an earthquake and avoid loss of life and property. Now, there have been a series of studies to determine and predict the exact time and location of an earthquake, but to a very little or no success at all. Given the conditions and deep seated locations of the occurrences of earthquakes, it becomes very difficult to provide a time frame long enough to deploy effective hazard management plans, though latest studies have bought us a window of about a minute by analyzing the fore-shocks of an earthquake. A very complex system of movement of tectonic plates and their interaction with the molten magma below the lithosphere govern the magnitude and strength of the earthquakes.

Numerous factors are known to cause earthquakes, some of them are:

- Tides
- Geothermal Energy
- Explosions
- Deforestation
- Landslides
- Climate change
- Surface quarrying
- Deep penetrating bombs
- Fracking
- Volcanic Activity
- Typhoons
- Silent slip
- Stress transfer
- Increase/decrease in pore pressure

Although it is difficult to accurately predict an earthquake, we can, however, try to determine the probability with which an earthquake can occur in a specific

zone given that we have sufficient data about the geology and the historic seismic activity of the area. Such an approach can help us deploy counter measures to timely help people seek shelter before any major catastrophe strikes.

The said approach is realized by mapping the zone wise chronological occurrence of earthquakes using 1, 4, and 8 bit fractal addressing system for a four cornered *chaos game*, and one-bit fractal addressing system for a six cornered *chaos game*, the details of which are discussed later.

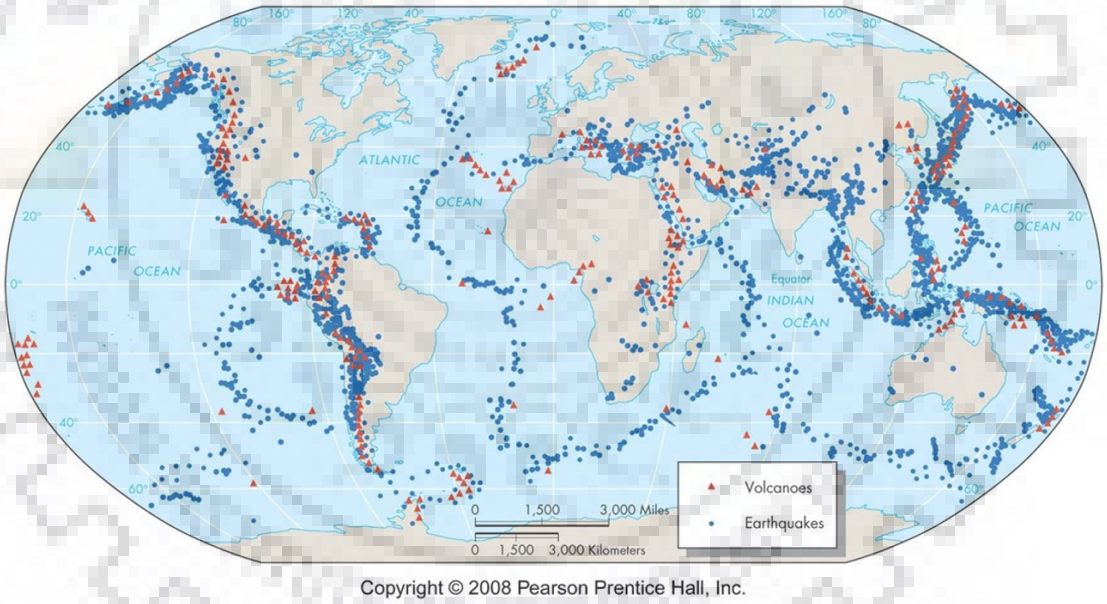

Figure 1.1: Location of Earthquakes and Volcanoes on Earth

Source: *https://clarkscience8.weebly.com/patterns-of-earthquakes-and-volcanoes.html*

Chapter 2

The Himalayas and the Andaman-Sumatra Region

2.1 Tectonic Setting of the Himalayas

Our understanding about the seismicity of the Himalayas has been broadly built upon paleoseismic records (like offset of frontal thrust faults), felt intensity reports and modern seismic data. But the Gorkha earthquake of 2015, $M_w = 7.8$, facilitated in interpreting many key aspects of some of the major earthquakes to occur in the Himalayan region. Nonetheless, it was not enough for us to gain new information on the convergence between the Indian and the Eurasian plates, and link the major and the great earthquakes $8<M_w<9$.

To determine the interval between subsequent occurrences of earthquakes in the Himalaya, the rate of convergence of the two plates is elemental. Although the Indian plate is quite rigid within a few millimeters (Paul et al. 1995; Banerjee et al. 2008; Jade et al. 2017), more that fifty per cent of the convergence is absorbed as internal deformation within the Asian continent, and results in reduced collisional velocity along the Himalayas. This velocity has been mostly determined indirectly through global plate-closure summations (Molnar Stock 2009), before GPS geodesy was available, and assuming there are no spreading centres between the two plates. Recent research work carried out by *Van der Voo et al. 1999; Jagoutz et al. 2015* has shown that due to the convergence of two nearly parallel, E-W subduction

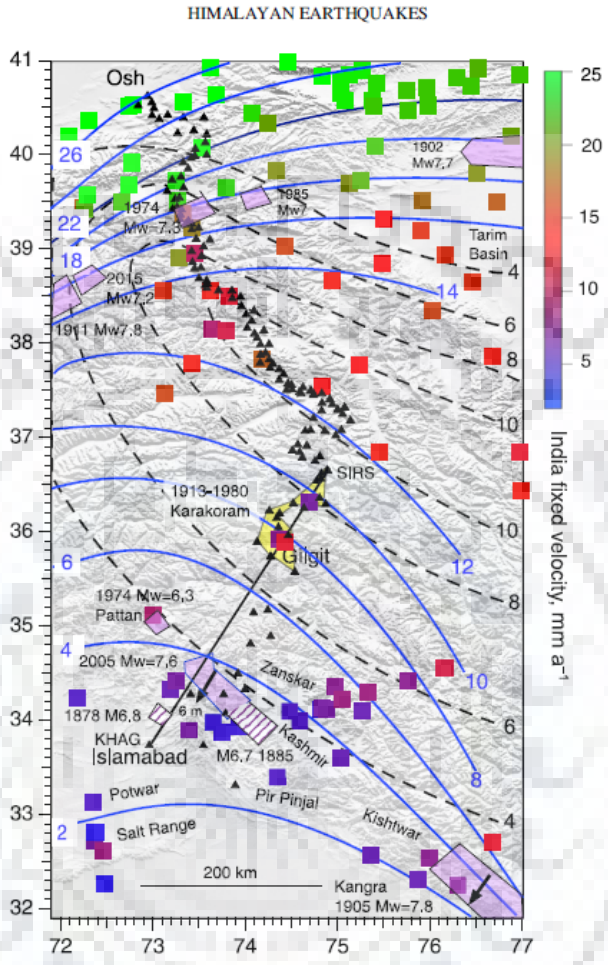

Figure 2.1: Historical geodesy; *small black triangles:* links the 19th century *Great Trigonometrical Survey of India* to the Russian Survey network (1913) (Mason 1914); *yellow:* a part of Indo-Russian network from Osh to Islamabad remeasured in 1980 (Chen et al. 1984); *blue solid and black contours:* indicate velocity in southwards & westward directions, respectively; *violet shading:* earthquake ruptures and their magnitudes.

Source: *https://sp.lyellcollection.org/content/early/2019/01/31/SP483.16*

zones, the Indian plate moved northwards at a rate of more than 14cm/year at 70-50 Ma BP, suddenly dropped down to a rate of 6 cm/year post closure of the Tethys ocean and the beginning of continent-continent collision at c. 50 Ma BP. The pole of rotation between the Indian Plate and the Eurasian Plate is currently considered to lie at 51.70 $\pm 0.3^0 N$, 11.85 $\pm 1.8^0 E$ (nearly 100 km SW of Berlin), with the convergence specified by an angular velocity of $0.553 \pm 0.006^0/Ma$ (Jade

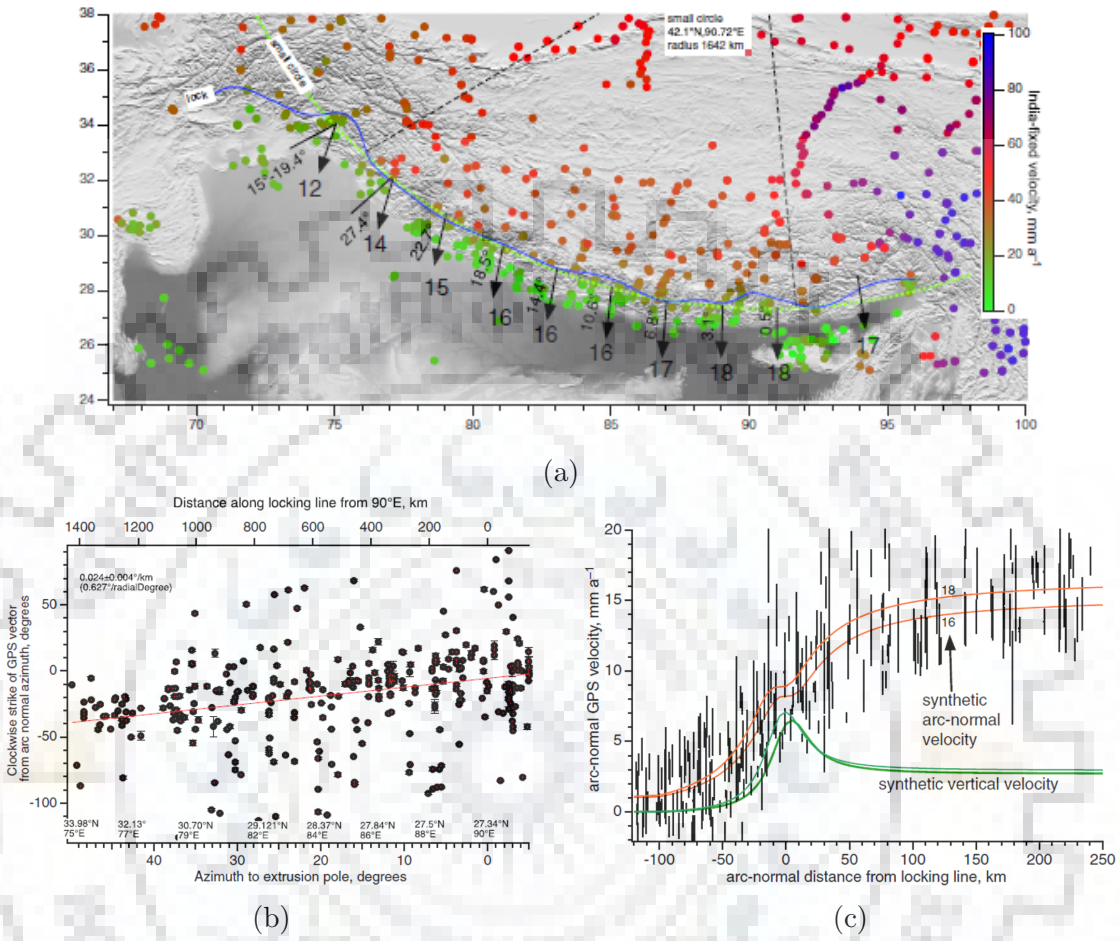

Figure 2.2: (a) India-fixed GPS north velocities outlined by Vernant et al. (2014) and Kreemer et al. (2014); blue line shows the 8.5 mm/annum velocity contour. (b) Deviation of GPS vectors (from arc normal). The red line determines the deviation from arc normal velocities. (c) Arc-normal velocities within the small-circle quadrant compared with synthetic velocities for a 6–9 dipping dislocation locked at 18 km depth, and with convergence velocities of 16 mm per year and 18 mm per year (red lines), and synthetic vertical displacements (green lines).

et al. 2017). Previous calculations with GPS data of lesser accuracy determined the position to be between Ireland and London, with uncertainty in the E-W position. It is said that the Indian plate rotates clockwise relative to Asia with c. 44mm/year of convergence near Pakistan, and 65 mm/year near Bangladesh. The rate of convergence reduces down to less than 18 mm/year across the Himalayas due to dispersion of convergence near Tibet and the northern mountains. The rate of convergence is less than 12 mm/year near the western Himalayas, around 17 mm/year near the central, and slows down in the east due to the clockwise

rotation of the Brahmaputra valley in contrast to the expected increase as a result of Indian plate's counterclockwise rotation. The Brahmaputra valley is a 300-km long segment of India that broke up from India at c. 5 Ma BP (Vernant et al. 2014).

2.2 Seismicity of the Himalayas

Seismicity surrounds the edges of the Indian plate and is prolific within the Tibetan Plateau, contrary to the virtually complete non-existence of earthquakes in the interior (Figure 2.3). Most of the earthquakes near the Himalayas occur at shallow depths (<30 km); with deep earthquakes recommending the descent of the Indian Plate into the mantle at the end of the arc. The lack of Benioff-Wadati zone, a characteristic of oceanic plate collisions, can be inferred from the relatively rare occurrences of of earthquakes exceeding the depths of 40 kms.

The convergence rate between the Indian Plate and the southern Tibet is key to determine an upper limit for the anticipated rate of seismic productivity for the Himalayas. The nearly 2000 km long and 100 km wide Main Himalayan Thrust accumulates seismic moment equivalent to a $M_w = 7.3$ earthquake, at a rate of c. 1020 N m/year (newton meters per year). Enough moment can be built up to generate earthquakes of magnitudes $M_w = 8$ and $M_w = 8.6$ in just 10 and 100 years respectively, while accumulation of over 350 years would be required to cause a 4 metre rupture of 2000 km length by an earthquake of $M_w = 9.0$.

The release of this potential slip is, however, irregularly placed along the lengths of space and time. Such irregularities result in slip deficits not only along the Himalayan arc, but around various plate boundaries around the world, in general. With the exception of aseismic slip, or creep, earthquakes occur to compensate for this slip deficits. Calculations show that a single large earthquake, say of $M_w = 7$ and rupture areas of about 100/50 km, would equal 30 such earthquakes of $M_w = 6$ in relieving the build up of this slip deficit, while a 1000 would equal the energy of $M_w = 8$. This justifies that in practical scenarios, only the largest of the earthquakes allow the Indian plate to move under the Tibetan Plateau, although several $M_w \leq 4$ earthquakes occur on a daily basis in the Himalayas. Only 3 major earthquakes have been documented in the Himalayan region since the seventeenth

century, $M_w = 8.2$ in 1897 (under the Shillong Plateau south of Bhutan), $M_w = 8.4$ in 1934, and $M_w = 8.6$ in 1950, while 8 have been recorded since 1600s between a range of $7<M_w<8$, out of which six have been known to occur since 1900 (1905, 1936, 1947, 2005 and two in 2015). One reason for such disparity in the latter could be incompleteness of the records, but that is highly unlikely given the region has fairly good coverage by the local administration, media reports, and accounts by local population.

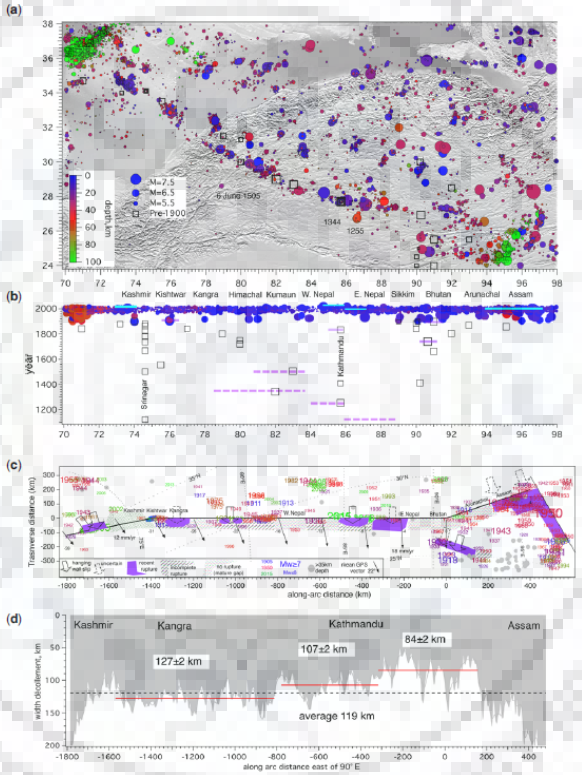

Figure 2.3: (a) Seismicity of Himalaya and Tibet. (b) Violet: rupture lengths of earthquakes since 19th century; dashed violet: inferred ruptures, and the spike in documented earthquakes since 1900; red for >40 km depth and blue for shallower. (c) Polar plot centred at 42.1^0N, 90.72^0E straightens the Himalaya and illustrates that the locking line closely follows a small circle. (d) Radial width of the decollement as a function of distance along the arc. The lower edge of the shaded region represents the Main Frontal Thrust; the upper edge the locking line. The red lines indicate along-arc spatial averages with their numerical values.

Source: *https://sp.lyellcollection.org/content/early/2019/01/31/SP483.16*

2.3 Tectonic Setting of the Andaman-Sumatra Region

According to McCaffrey (1992) Andama & Nicobar subduction system situated at latitude 5–15^0N , known as one of the most seismically active regions on Earth near the sunda subduction zone the Indian Plate subducts beneath the Eurasian Plate in a nearly arc-parallel direction, @ 43 mm/year. After the cretaceous period the plate convergence increased significantly. The collision of the Indian Plate with Eurasia has played a key role in the tectonic evolution of the region and the present day configuration of the subduction zone.

In the north, the north–south trending Andaman–Nicobar subduction system joins with its onshore prolongation, the Indo-Burmese arc 17–27^0N. At the intersection Sumatra-Andaman and the Indo subduction zone, basically the Burmese range, is way more sophisticated and the seismic activity in this region is more. It is found that there is slip partitioning in the Indo-Burmese arc and on the Sagaing Fault. The stress state across the region does not support the subduction across the Indo-Burmese arc at present while subduction is more pronounced along the Andaman–Nicobar system.

Supported by the historical events along the Andaman–Nicobar there were two events one being the 1881 (M_w = 7.9) and 1941 (M_w = 7.7). Also, two events were recorded (M_W>7) since December 2004. These earthquakes occurred in the subducting plate and were generated by left-lateral strike-slip faulting on NNE–SSW oriented near-vertical faults.

2.4 Seismicity of the Andaman-Sumatra Region

There are three major frequency magnitude distribution for the classification of Sumatra-Andaman Subduction Zone (SASZ): (i) probability of maximum magnitude earthquake, (ii) recurrence or return period, and (iii) probability of occurrence of all type of earthquake.

Close to the western coast of Myanmar and southern southern Nicobar, SASZ is known to have the capability to generate a $M_w = 6.1-6.4$ magnitude earthquake in the next three to five decades, while the "high hazard region" south of the north-

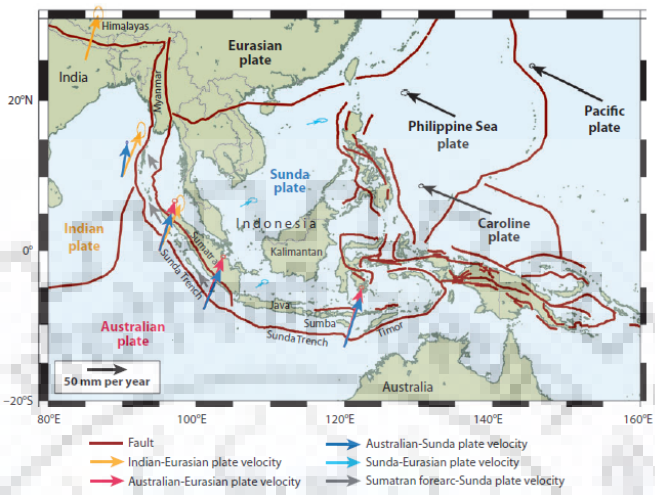

Figure 2.4: Plate tectonic setting of the Andaman-Sumatra region.

Source: *Robert McCaffrey (2008)*

western and western parts of Sumatra has a shorter return period as compared to other regions, 6-12 and 10-30 years for earthquakes of magnitudes $M_w = 6.0 or 7.0$, respectively.

There's an almost 100 per cent probability for an earthquake with M_w up to 6.0 to occur in the area along the SASZ in the next half a century, whereas a less than 50 per cent chance for a $M_w = 7.0$ earthquake in the same period of time. Also, in the next 50 years, there's a 90 per cent chance of a $M_w = 6.0$ earthquake in the areas near the city of Yangon despite them being labelled as the least hazardous in the proximity of SASZ. Hence, an effective mitigation plan of sesimic hazard should be in place.

Chapter 3

Methodology

3.1 Fractals

A *fractal* is a curve or geometric figure with the same statistical character in each part as the whole. They are useful in modeling structures (for example, snowflakes), in which similar kind of patterns recur at gradually smaller scales, and in describing partially random or chaotic phenomena such as the formation of crystals and galaxies.

Benoit Mandelbrot described geometric fractals as "a rough or fragmented geometric shape that can be divided into parts, each of which is (at least roughly) a copy of the whole"; in general, this is useful but limited. Most people usually diverge when it comes to decide on a single definition of *fractals*, but often reinforce the basic proposal of self-similarity and the distinctive correspondence fractals share with their surrounding space.

Nevertheless, the point everyone agrees on is that the fractal patterns are governed by fractal dimensions, although the dimensions neither specifically describe nor define the details of how to construct a particular fractal pattern, but quantify the complexity of the fractal, such as changing detail with changing scale. The word "fractal" was coined by

Mandelbrot, a Polish born French-American mathematician, first suggested the word "fractal" in 1975, to describe an object whose Hausdorff – Besicovitch dimensions exceeds its topological dimensions. However, it has been noted that space-filling curves such as the Hilbert curve do not meet this requirement.

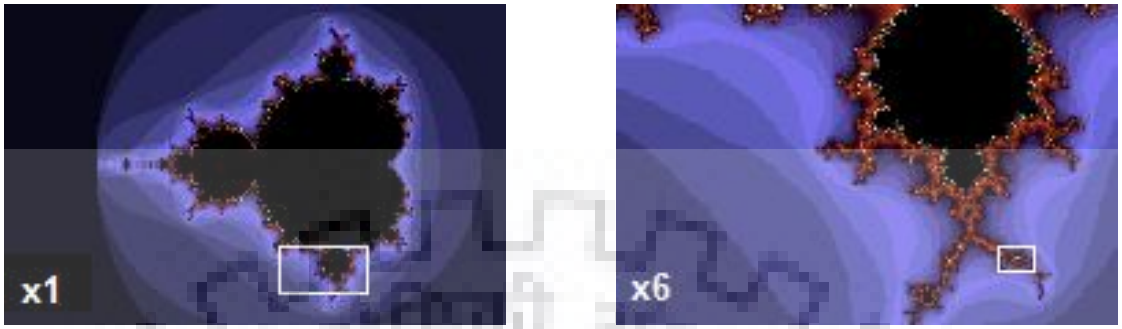

(a) Mandelbrot set; this panel has no magnification.

(b) At 6-fold magnification similar patterns can be observed

(c) 100-fold magnification of the same fractal as (a)

(d) Even at 2000-fold magnification, the Mandelbrot set resembles the details at zero or lower magnifications

Figure 3.1: Self-similarity of fractals illustrated with an example of *Mandelbrot Set*

Source: *h*ttps://commons.wikimedia.org/wiki/File:Mandelbrot-similar-x1.jpg

Since the scientific community does not have a unanimous stand on a singular definition for fractals, many argue that as such it shouldn't be defined strict at all. According to Falconer, a fractal should be defined only generally by the following characteristics, along with being non-differentiable and capable of having a fractal dimension:

- Self-similarity, which may consist:
  - *Exact self-similarity*: perfectly identical at every scale, such as the Koch curve
  - *Quasi self-similarity*: approximately the exact pattern at various scales; may include smaller duplicates of the whole fractal in degenerate and distorted form; for example, Mandelbrot set's satellites are not exact copies, but approximations of the entire set

  - *Statistical self-similarity*: stochastic recurrence of patterns such that numerical and/or statistical measures are maintained across different scales; the coastline of Britain is a well know example of randomly generated fractals for which one wouldn't expect a segment to be neatly scaled and repeated
  - *Qualitative self-similarity*: like in a time series
  - *Multifractal scaling*: generally defined by multiple fractal dimensions or scaling rules.
- Detailed arbitrarily small-scale structure. This structure may result in fractals having emerging properties.
- Locally and global irregularities that are not easily described in traditional Euclidean geometry. This has been expressed, for images of fractal patterns, by expressions such as "smoothly piling up surfaces" & "swirls upon swirls".

Together, the criteria listed above lay basis to not include instances of self-similar but without the typical fractal features. For example, a straight line is not a fractal despite being self-similar at all scales as it lacks details, is describable in Euclidean geometry, possess the same Hausdroff - Besicovitch dimension as its topological dimension, and can be completely defined without recurrence.

3.1.1 Techniques for generating fractals

Fractal generating programs can be deployed to create fractal images. It is important to note that because of the *Butterfly effect*, unprecedented outcomes may be observed as a result of even a very tiny change in a single variable.

- *Iterated function systems (IFS)* – it uses established rules for geometric replacement; could either be stochastic or deterministic; for example, Harter-Heighway dragon curve, T-square, Haferman carpet, Sierpinski carpet, Sierpinski gasket, Peano curve
- *Strange attractors* – it uses solutions of a system of initial value differential or difference equations that manifest chaos (e.g., multifractal image)
- *L-systems* – it makes use of string rewriting; may imitate branching patterns, such as in blood vessels, pulmonary structures, plants, biological cells etc.

- *Escape-time fractals* – it uses a formula or recurrence relation at every point in space (such as the complex plane); usually quasi self-similar; also called "orbit" fractals; for example, the, Burning Ship fractal, Nova fractal Lyapunov fractal and Julia set. The 2-D vector fields, generated by one or two iterations of escape-time formulae also result in a fractal form where points (or pixel data) are passed through the field repeatedly.
- *Random fractals* – it uses stochastic rules; for example, percolation clusters, fractal landscapes, Lévy flight, trajectories of Brownian motion and the Brownian tree (i.e., dendritic fractals generated by reaction-limited aggregation clusters or by modeling the diffusion-limited aggregation).

3.2 Iterated Function Systems

Iterated Function System, introduced in 1981, is a way of generating fractals, which are mostly self-similar.

IFS fractals are usually caqlculated and drawn in 2-D, but can exist in any number of dimensions. They are made up of a culmination of a number of replicas of themselves, each replica being modified by a function (hence *"function system"*). The prime example being the *Sierpiński triangle*. The iterated function systems are generally contractive, meaning they move the points closer together and subsequently create smaller and smaller shapes. As a result, an IFS fractal is made up of several, and probably overlapping, smaller replicas of itself, each of which, in turn, is also made up of replicas of itself, ad infinitum. This is the reason for IFS fractal's self-similar nature.

Using ietrated function systems, a *Sierpiński triangle* can be formed using the function below:

1. Let the total number of iterations be i.
2. Let the total number of transformations possible be n.
3. Tag every transformation with an integer starting from 1 to n.
4. Pick any point at random, say a.
5. Generate an arbitrary integer from 1 to n.
6. Apply the transformation tagged by that arbitrary integer to a to generate a new point a.

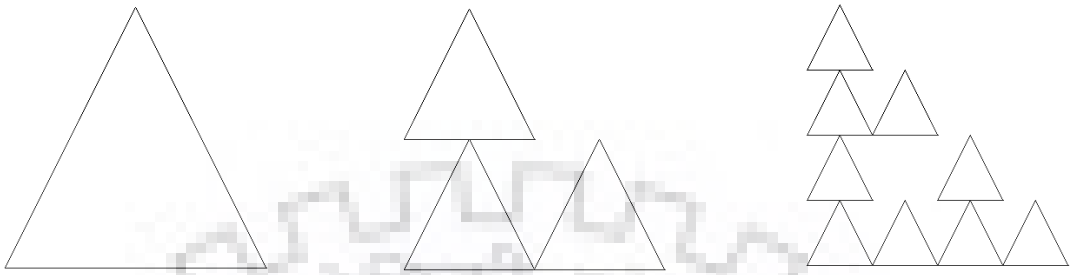

(a) Without iteration (b) Iteration #1 (c) Iteration #2

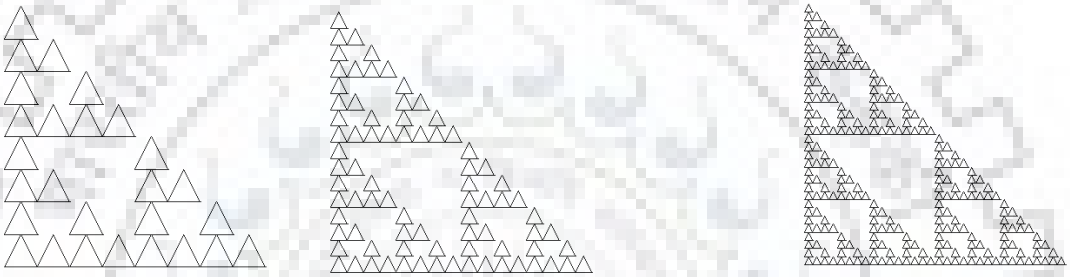

(d) Iteration #3 (e) Iteration #4 (f) Iteration #5

(g) Iteration #6 (h) Iteration #7

Figure 3.2: The Sierpinski Gasket at various iterations

Source: http://pages.cs.wisc.edu/ergreen/honorsthesis/anisierpinski.html

7. Plot *a*.
8. Go to step #5, repeating it i times.

3.3 Chaos Game Representation

Chaos Game Representation (CGR) is an iterated function that bijectively maps discrete series into a continuous domain. As a result, a discrete series can become an object of statistical and topological analysis, which is otherwise reserved to numerical systems.

Chaos Game Representation (CGR) was originally proposed by Jeffrey in 1990 (Jeffrey, 1990), as a representation for genomic sequences, without any dependencies on the scale. Formally an iterative function system, the CGR technique can be trailed back to the premise of statistical mechanics to Chaos theory, in particular (Bar-Yam, 1997).

By playing the Chaos Game for *Human Beta Globin*, Jeffrey observed the following patterns:

- the upper right quadrant (the g-quadrant) there is almost empty
- the left (c-quadrant), there's a double scoop appearance
- the CGR of Human Beta Globin follows self-similarity and its features are also found in several other genetic sequences.

The last point, especially, affirmed the credibility of application of CGR (and Iterated Function System) to better understand and study various natural phenomena such as actin cytoskeleton, crystals, DNA, geometrical optics, and *earthquakes*.

In mathematics, the term chaos game, given by Michael Barnsley (1988), used a polygon and an arbitrary point inside of it to generate a fractal.
In simpler terms, it proceeds as follows:

1. Mark 3 non-collinear points and label them as X, Y, and Z.
2. Mark another arbitrary point anywhere on the same plane. This becomes the *current point*.
3. Now roll a six sided die. If 1 or 2 is the number which appears on top, then plot the midpoint between the current point and A. If 3 or 4 is number, then plot the same between B and the curent point, and towards C if the number is either 5 or 6. In each iteration, the last plotted point becomes the current point.
4. Repeat the step 3.

For a large number of iterations of the above steps, one might expect random

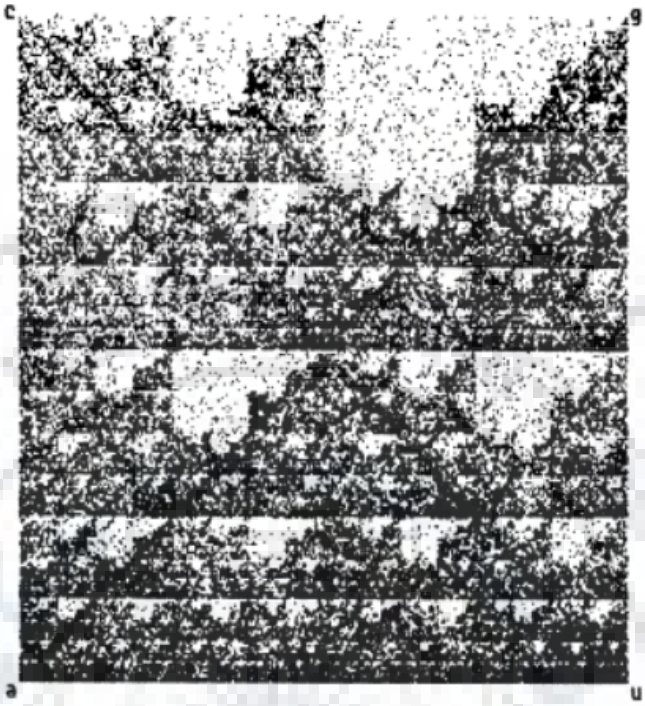

Figure 3.3: CGR of Human Beta Globin Region on Chromosome 11 (HUMHBB) (73,357 bases)

Source: *Chaos Game Representation of Gene Structure by H Joel Jeffrey*

dots to completely fill the paper, or perhaps a triangle. However, such is not the case. What we obtain is a triangle subsequently filled with scaled copies of smaller triangles. The figure, thus obtained, is called the *'Sierpinski Gasket'*, as discussed earlier, named after the mathematician who first defined it. Though, for an even sided polygon, we obtain a completely filled polygon for a random sequence such as explained in the steps above.

3.4 Methodology

For the purpose of this thesis, Iterated Function Systems are used, and fractal images of earthquakes are generated by playing Chaos Game. The said method is approached in two separate manners:

1. Fractal images of 1, 4, and 8 bit fractal addresses are generated by playing a

four-cornered chaos game

2. Single bit fractal images are generated by playing six-cornered chaos game.

While generating fractals images, it is important to determine the fractal address of a given point within the defined spaces. A fractal address can be defined as 1, 2, 3, 4.... bits and so on, depending upon the scale at which the fractals are generated; the longer the fractal address, the smaller the portion that it denotes and the more detailed the visualization. For programming purposes, each address points towards a specific bin, whose value gets incremented each time that address is called. For example, given a random sequence of characters, the fractal addresses can be defined as follow:

Random sequence: 11254236525522333245124442525233623622 2.....

- **1-bit addresses:** 1; 1; 2; 5; 4; 2; 3; 6; 5; 2; 5; 5...and so on
- **2-bit addresses:** 11; 25; 42; 36; 52; 55...and so on
- **3-bit addresses:** 112; 542; 365; 255....and so on
- **4-bit addresses:** 1125; 4236; 5255...and so on

For example, fractal address can be mathematically generated using the following transformations:

$T_3(x,y) = (x/2, y/2) + (0, 1/2)$	$T_4(x,y) = (x/2, y/2) + (1/2, 1/2)$
$T_1(x,y) = (x/2, y/2)$	$T_2(x,y) = (x/2, y/2) + (1/2, 0)$

These transformations will generate a filled-in unit square, S.

$$S = T_1(S) \cup T_2(S) \cup T_3(S) \cup T_4(S)$$

To each of the 1/2 x 1/2 square $T_i(S)$, an address of length '1' (say, i) is associated, i.e., a 1-bit address.

Each of these squares can be further divided by iterating this decomposition process as follows:

$$T_1 S = T_1 T_1(S) \cup T_1 T_2(S) \cup T_1 T_3(S) \cup T_1 T_4(S)$$

associating a length 2 address (say, ij) to each 1/4 x 1/4 square, and so on.

In application, fractal addresses are read right to left: the left-most digit being the index of the most recent transformation applied.

(a) 1-bit addresses

(b) 2-bit addresses

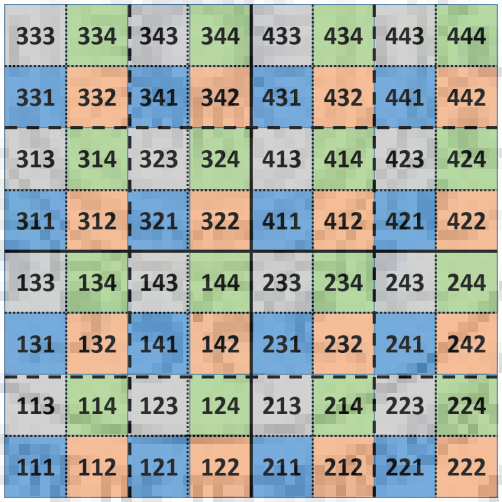

(c) 3-bit addresses

Figure 3.4: Representation of fractal addresses as 1-bit, 2-bit, and 3-bit addresses

Chapter 4

Data and Area of Study

4.1 Data

For the purpose of this thesis, earthquake data was downloaded from the official website of the *United States Geological Survey* (https://earthquake.usgs.gov/earthquakes/search/). The data consists of earthquakes above a magnitude of 3.5, starting 01-January-1970 00:00:00 hours till 31-December-2018 23:59:59 hours. All the data between latitudes -10^0S and 50^0N, and longitudes 50^0E and 110^0E was downloaded, which was then divided into separate zones as per the requirement.

The coarse grain magnitudes, highlighted in the image above, are important to generate fractal images of varied bit addresses.

For both four and six-cornered chaos game, the area of study was divided into respective number of zones according to their geographic location, putting together areas of similar geological features.

For four-cornered chaos game, the area is divided in the following manner:

ZONE NAME	Lat (N)	Lat (S)	Long (W)	Long (E)
Kashmir Himalayas	39.5	33	69	74
Nepal Himalayas	39.5	27	74	89
North-Eastern Himalayas	38.5	21	89	104
Andaman-Sumatra Region	21	5	91	96.5

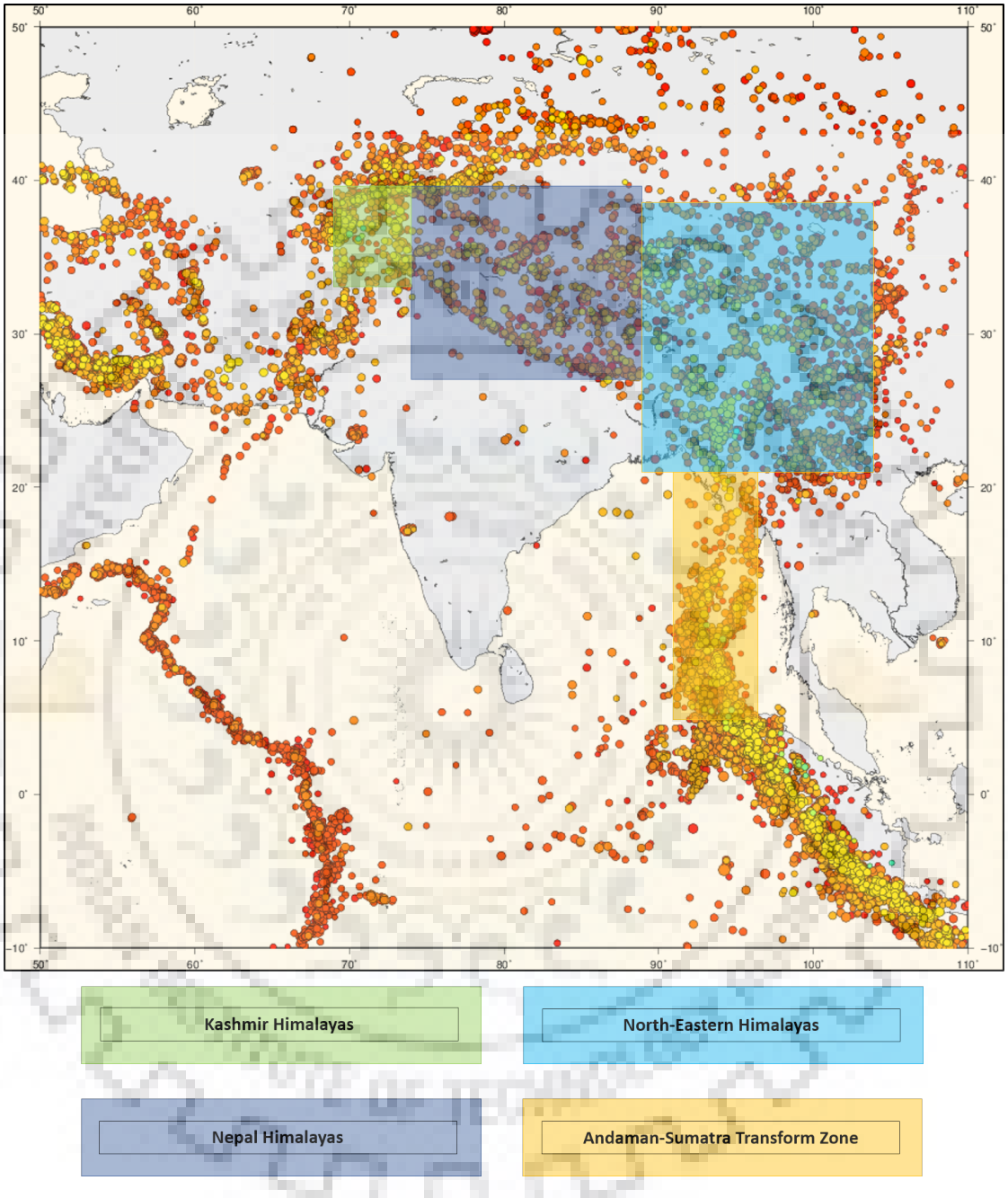

Figure 4.1: Division of study area for four-cornered chaos game

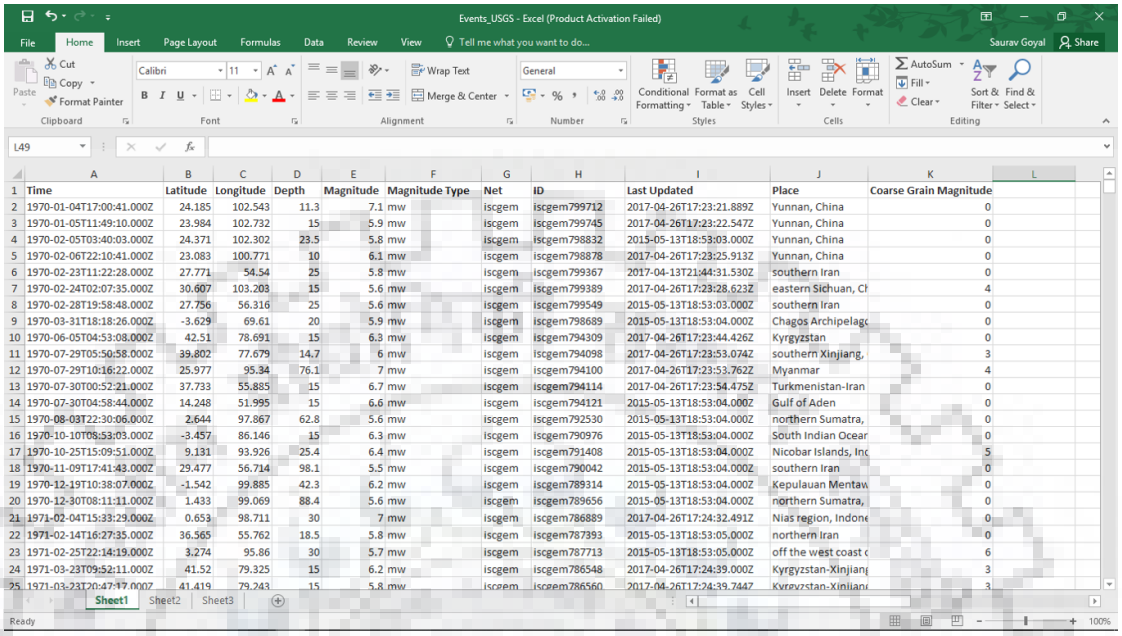

Figure 4.2: A sample of earthquake data set

For six-cornered chaos game, the area is divided in the following manner:

ZONE NAME	Lat (N)	Lat (S)	Long (W)	Long (E)
Gujarat Transform Region	42.5	22.5	64	71
Kashmir Himalayas	42.5	35	71	76
Nepal Himalayas	42.5	25	76	89
North-Eastern Himalayas	42.5	25	89	105
Andaman-Sumatra Convergence	25	10	94	95
”	25	5	90	94
Andaman-Sumatra Transform	25	10	95	97
”	10	0	94	97

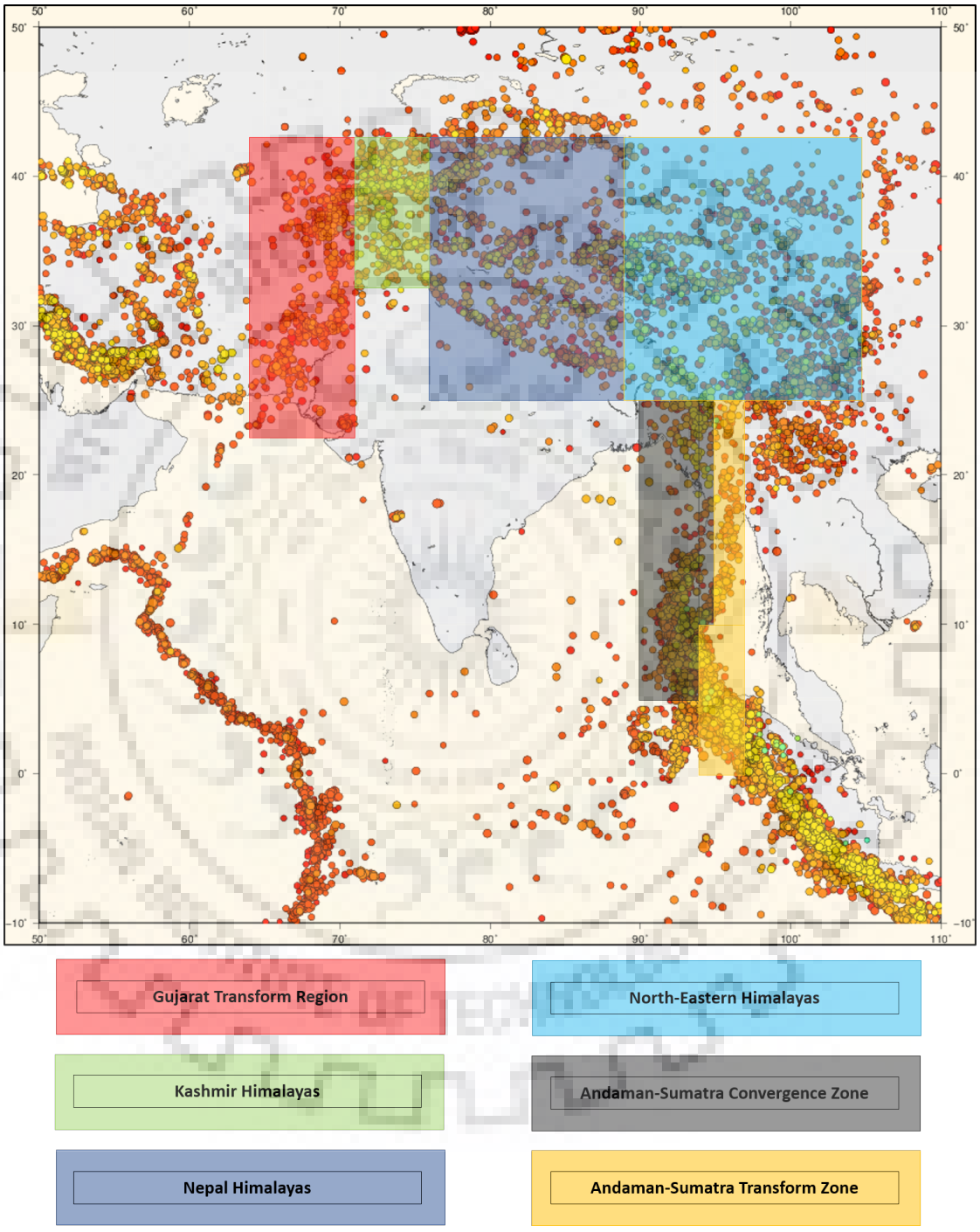

Figure 4.3: Division of study area for six-cornered chaos game

Chapter 5

Results & Discussion

The fractal images produced as a result of the procedure in the previous chapter shown below.

5.1 Results

5.1.1 Four-cornered Chaos Game

While playing the four-cornered chaos game, the 4 different zones can be arranged around the quadrilateral in 4! ways, i.e., 24 ways, but the number of unique arrangements is just 6. The results for these six cases for 1, 4, and 8 bit fractal addresses are as shown in the subsequent figures (Figure 5.1 - Figure 5.6).

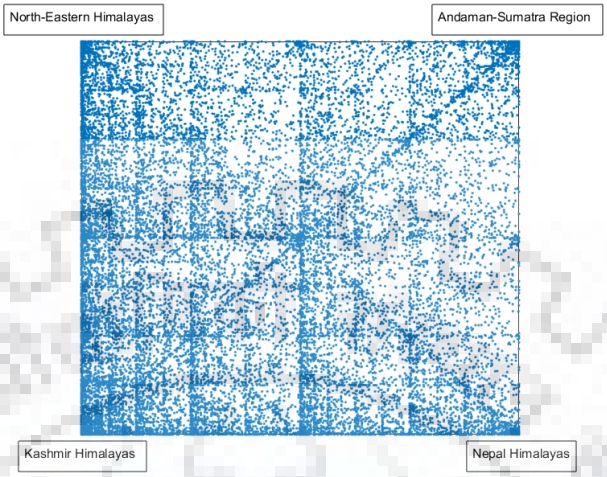

(a) 1-bit Image

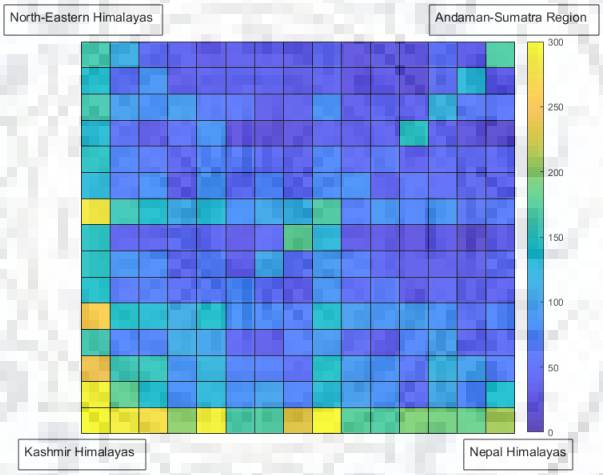

(b) 4-bit Image

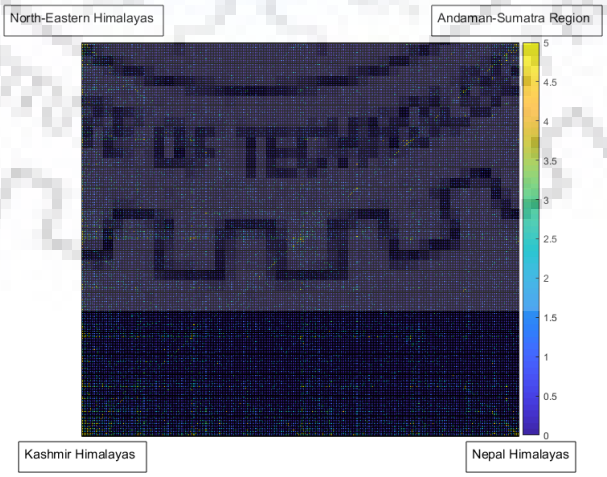

(c) 8-bit Image

Figure 5.1: Fractal Images for the arrangement type A B C D

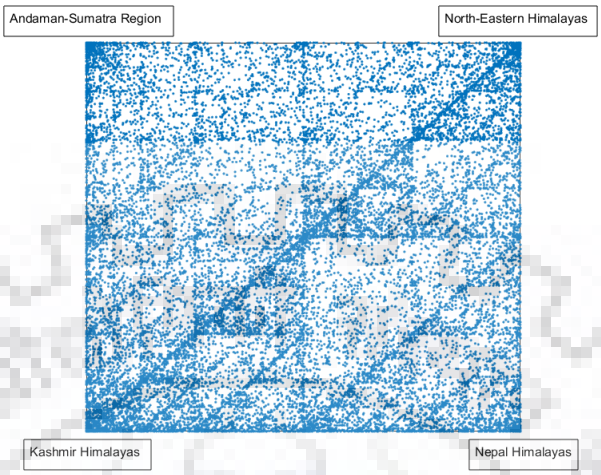

(a) 1-bit Image

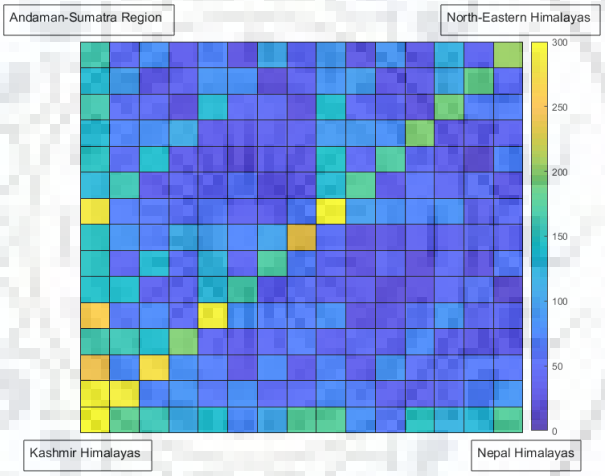

(b) 4-bit Image

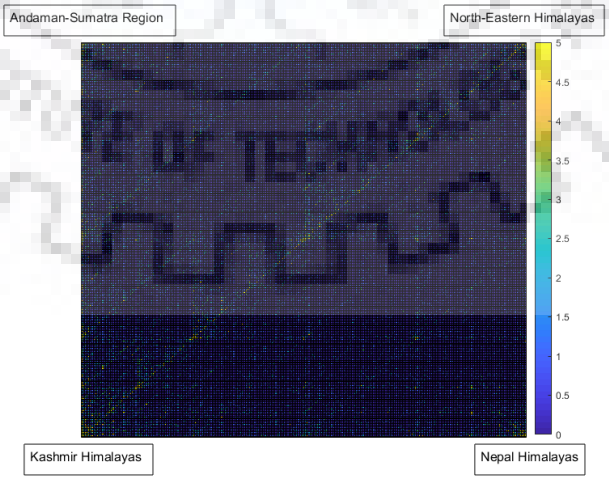

(c) 8-bit Image

Figure 5.2: Fractal Images for the arrangement type A B D C

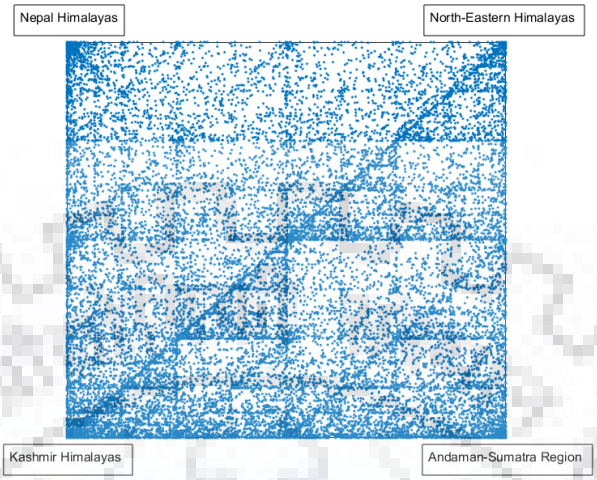

(a) 1-bit Image

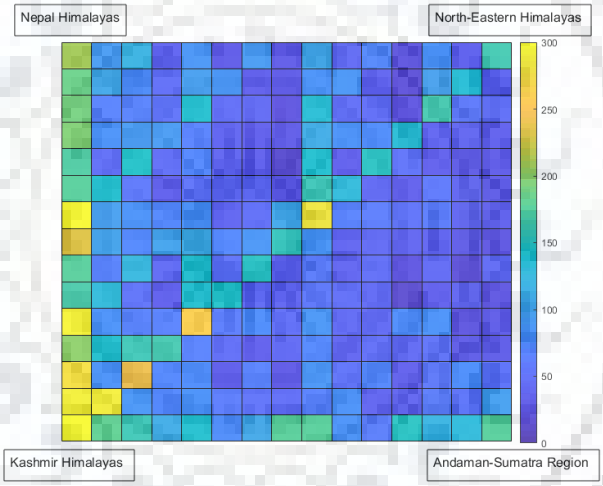

(b) 4-bit Image

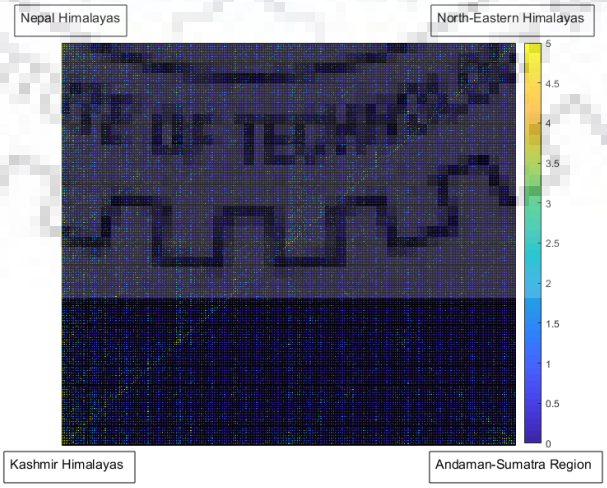

(c) 8-bit Image

Figure 5.3: Fractal Images for the arrangement type A D B C

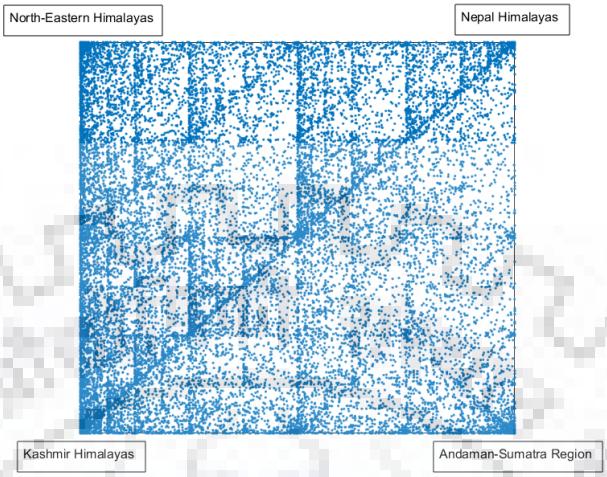

(a) 1-bit Image

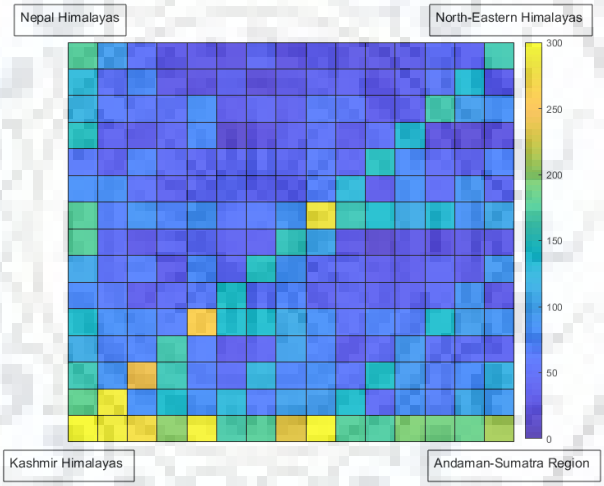

(b) 4-bit Image

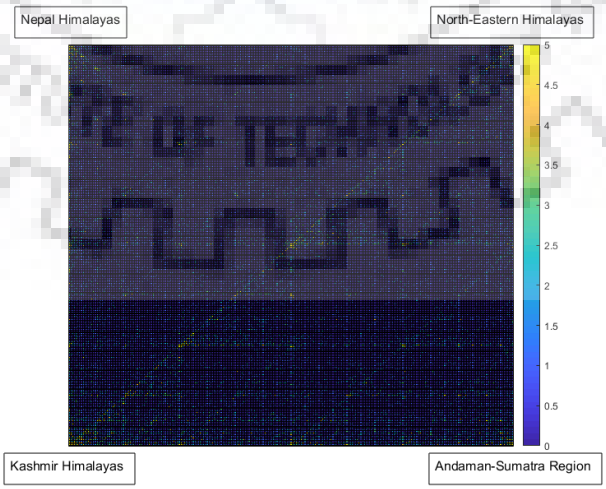

(c) 8-bit Image

Figure 5.4: Fractal Images for the arrangement type A D C B

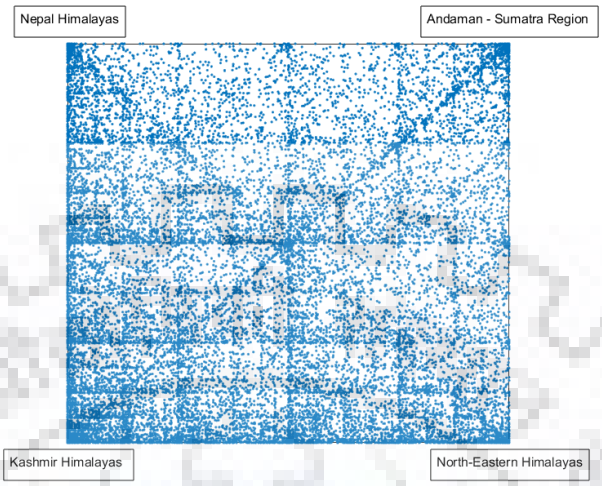

(a) 1-bit Image

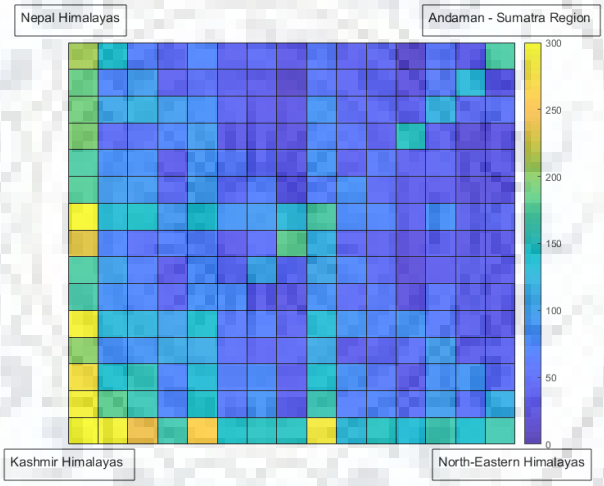

(b) 4-bit Image

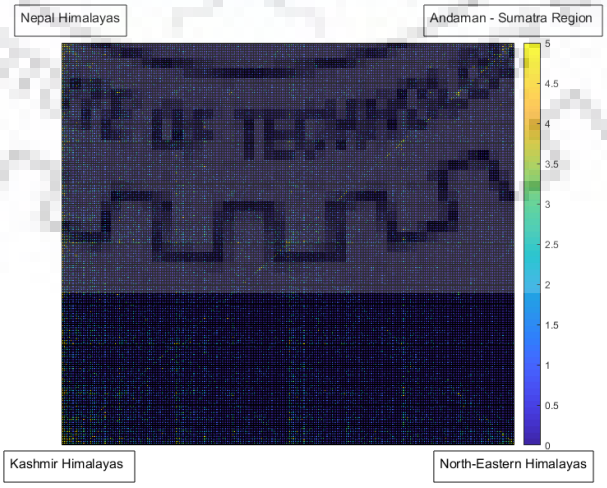

(c) 8-bit Image

Figure 5.5: Fractal Images for the arrangement type A C B D

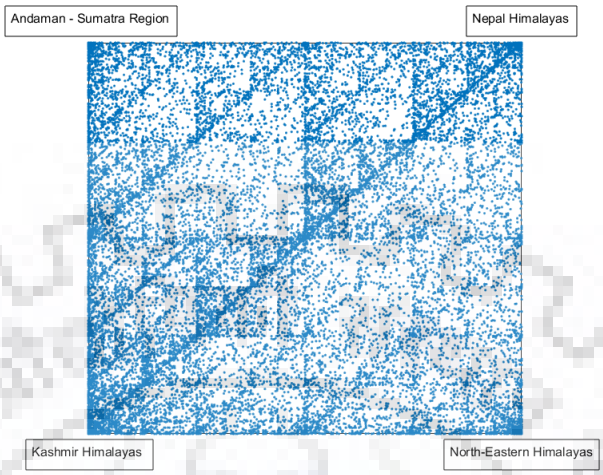

(a) 1-bit Image

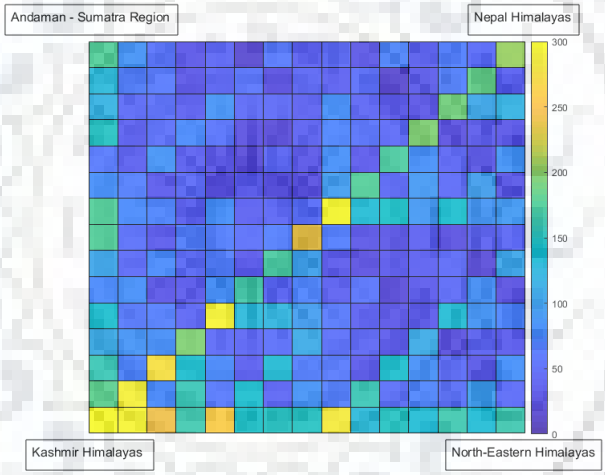

(b) 4-bit Image

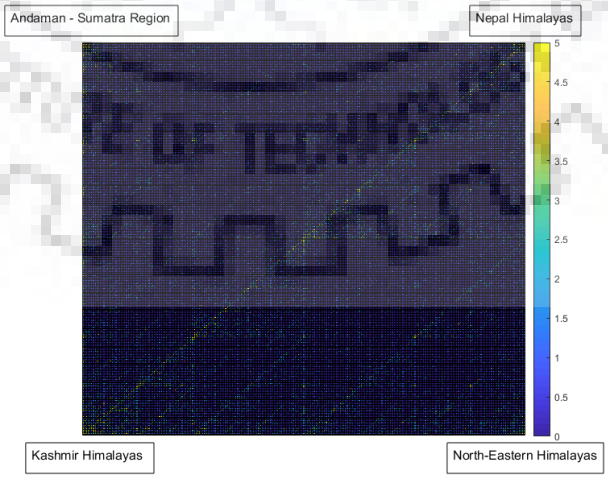

(c) 8-bit Image

Figure 5.6: Fractal Images for the arrangement type A C D B

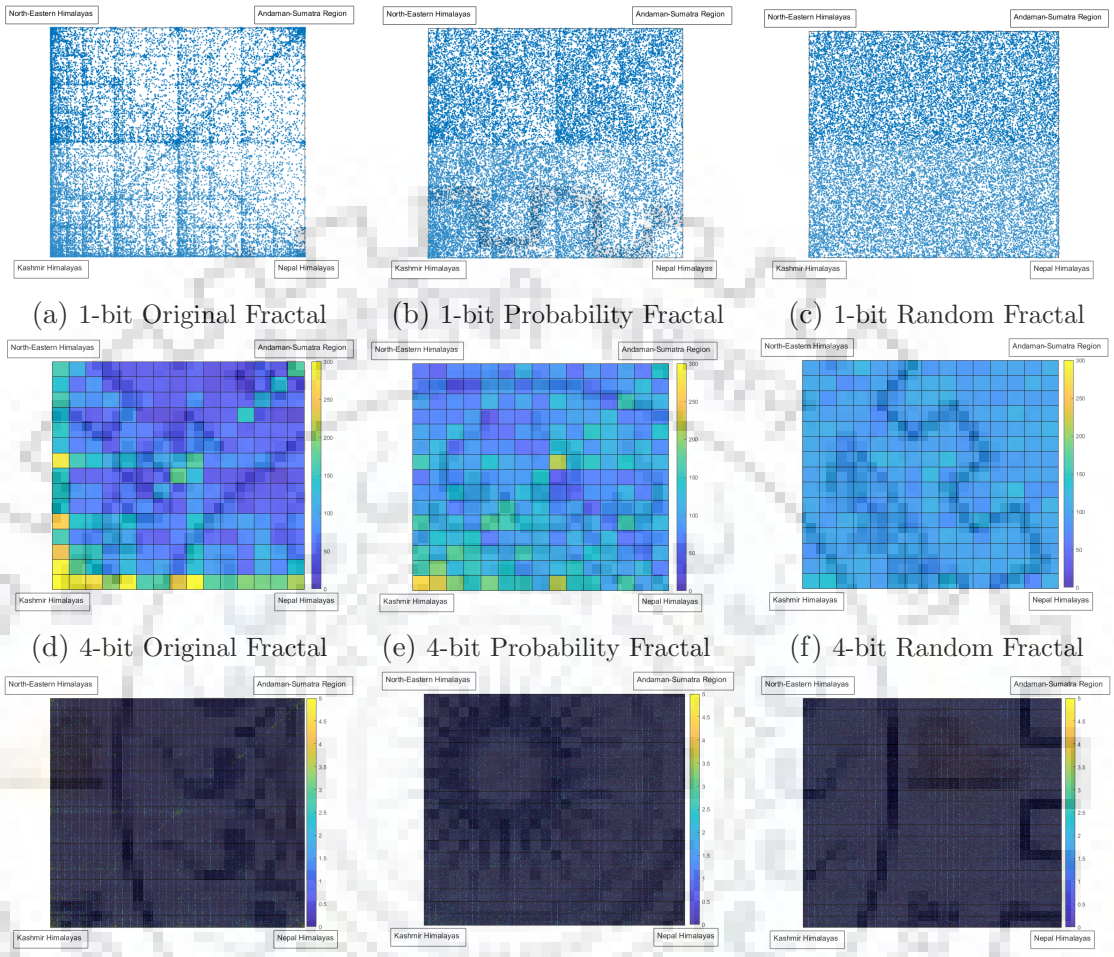

(a) 1-bit Original Fractal (b) 1-bit Probability Fractal (c) 1-bit Random Fractal

(d) 4-bit Original Fractal (e) 4-bit Probability Fractal (f) 4-bit Random Fractal

(g) 8-bit Original Fractal (h) 8-bit Probability Fractal (i) 8-bit Random Fractal

Figure 5.7: Variations in fractal images generated using the actual data, the probability data, and a random sequence for the *Case 1: A B C D*

5.1.2 Six-cornered Chaos Game

The results for the six-cornered chaos game are illustrated below in Figure 5.7. Along with the fractal image of the actual data of the earthquakes, fractal image for probability distribution (assuming events in each each zone to be independent of the other), and the fractal image for a random sequence of numbers between 1 to 6, donating each zone, and assigning equal probabilities. A random sequence of numbers, with equal probabilities, should fill in the hexagonal space within the boundaries, as shown in Figure 5.7 (c).

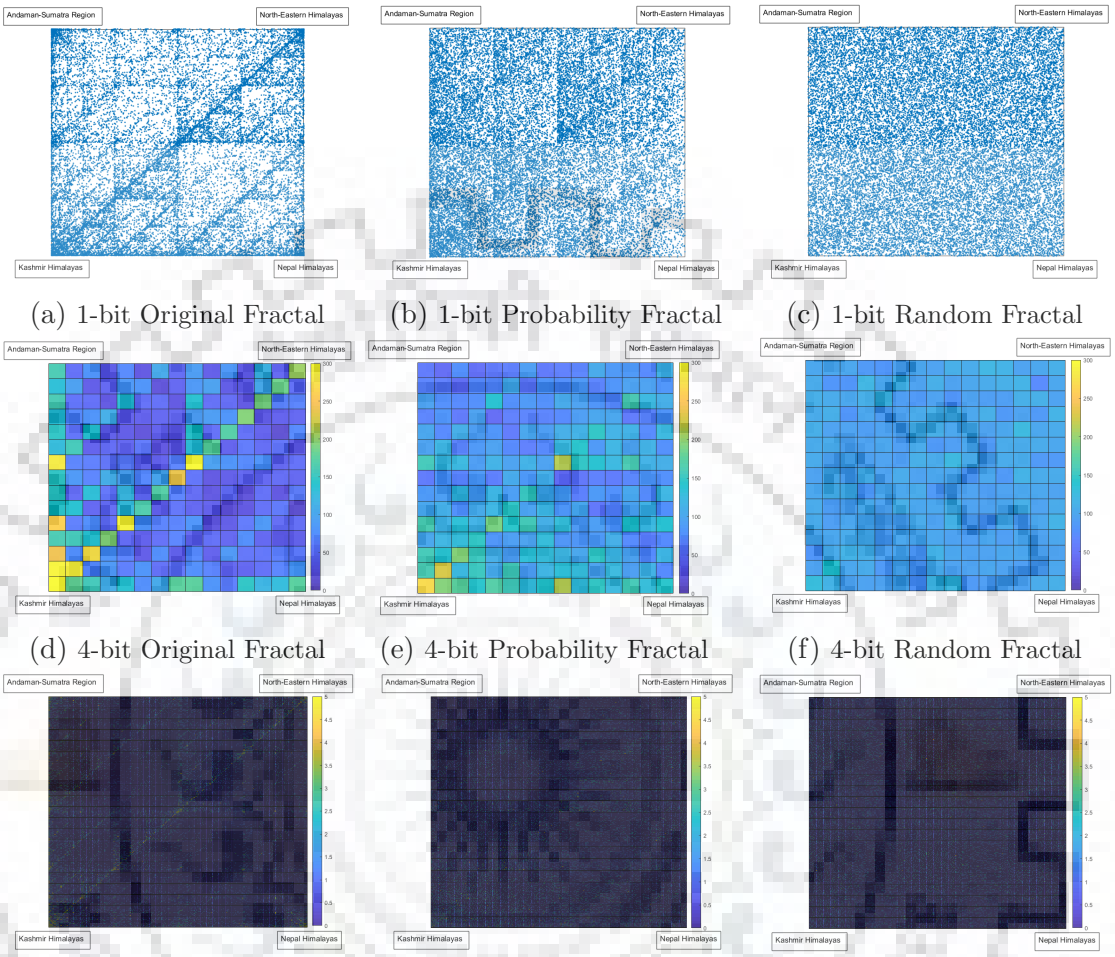

(a) 1-bit Original Fractal (b) 1-bit Probability Fractal (c) 1-bit Random Fractal

(d) 4-bit Original Fractal (e) 4-bit Probability Fractal (f) 4-bit Random Fractal

(g) 8-bit Original Fractal (h) 8-bit Probability Fractal (i) 8-bit Random Fractal

Figure 5.8: Variations in fractal images generated using the actual data, the probability data, and a random sequence for the *Case 2: A B D C*

5.2 Discussion

The results shown in the above sections, Figures 5.1 (a), 5.2 (a), 5.3 (a), 5.4 (a), 5.5 (a), 5.6 (a), and 5.7 (a), illustrates that a correlation must exist between the zones plotted. As a proof, fractals generated by the actual data, probability of occurrence of each event independently, and a random sequence of numbers generated with equal probability are plotted side by side in Figures 5.7 and 5.8 for four-cornered, and in Figure 5.9 for six-cornered chaos game. The probabilities for events in each zone are calculated by dividing the total number of events in respective zones to the total number of events in the considered data set.

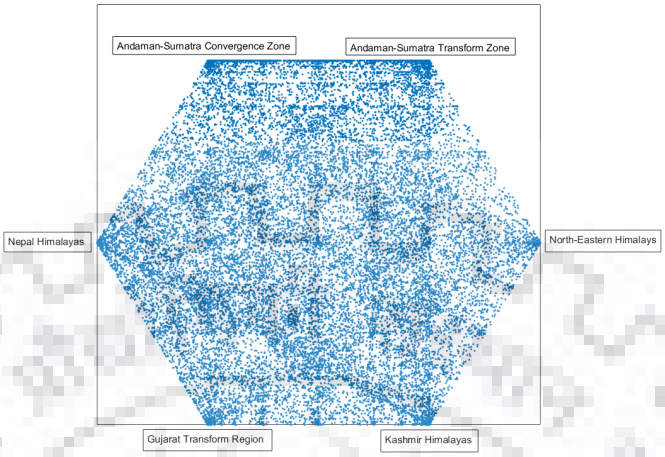

(a) Fractal image for the earthquake data

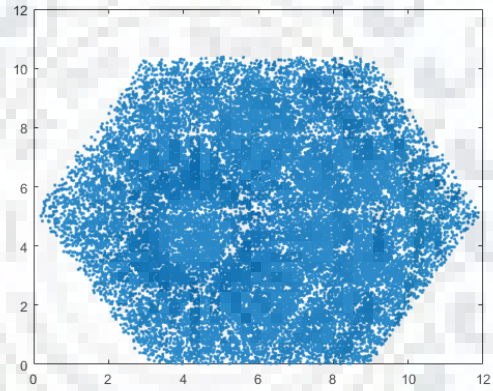

(b) Fractal image of the probability distribution assuming each event to be independent of the other

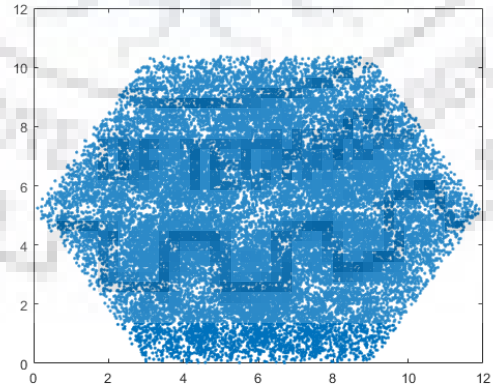

(c) Fractal image for a random sequence of numbers 1-6 generated with equal probability for each

Figure 5.9: Comparison of fractal images generated by playing six-cornered chaos game for the actual data, its probability distribution, and a random sequence

As can be seen in the images, it is observed that the original fractals exhibit some sort of pattern and do not look like their random counterparts. Even the fractals generated by their respective probabilities show a different trend. Therefore, the idea of any sort of randomness can be eliminated and it would be safe to assume that the earthquakes in different zones are somehow related.

However, a close inspection of the probability fractals and the random fractal for the six-cornered chaos game reveals a different story. It can be observed that both the fractal images display strikingly similar patterns. It can lead to the conclusion that the vents are indeed independent of each other, and there must not exist a correlation between them. Nonetheless, this is in contrast to their four-cornered counterparts displayed in the Figures 5.8 and 5.9.

One possible reason behind this contradictory result could be the lack our knowledge and understanding of fractals and their behaviour for six-cornered chaos game. Negligible studies have been carried out in this regards. Therefore, the observation could possibly be a result of one of the characteristic of this sort of fractal patterns. Another possibility could be lack of more variables. These images were generated using just a time series sequence of the earthquake events. Other factors such as the local geological conditions, length and orientation of earthquake ruptures, location of hypocentres etc. may influence the correlation, and effect the probabilities.

The similarity between the probability and the random fractals isn't just established qualitatively, but also by quantitatively by deploying appropriate machine learning models. The maximum dependencies are obtained for the conditions like $P(A|B)$, the highest being that for $P(2|2) = P(6|6) = 6.3\%$, and for $P(A|A)$, in general. For events in different zones, the highest value that the model returned is $P(2|1) = 3.7\%$. Here, '1' denotes earthquakes occurring in the *Gujarat Transform region*, '2' denotes the *Kashmir Himalayan region*, and '6' denotes the *Andaman-Sumatra Transform region*. It is also worth mentioning that Figure 5.10 signifies that the probabilities $P(A|B)$ and $P(B|A)$ are nearly equal, i.e., the probability of occurrence of $'B'$ after $'A'$ is nearly equal to that of $'A'$ after $'B'$.

Figure 5.10: Conditional probabilities obtained for six-zone study of earthquakes

Chapter 6

Conclusion

The following conclusions can be drawn from this work:

- Fractals, while being an important part in the research carried out in other fields such as the study of the genomes and DNAs, can also play a key role in the study of the earthquakes.
- The qualitative analysis of fractal representation of earthquakes in the Gujarat Transform Region, the Himalayan ranges of Kashmir, Nepal, and North-Eastern India, and the Andaman-Sumatra Region exhibit some sort of correlation between them.
- It implies that the occurrence of an earthquake in one region must affect the other.
- But contrary to the above statement, quantitative analysis of the data indicate very little dependencies between the zones, considering the limits of the data set used.
- Such contradiction must be clarified and require further studies using extra variables, such as, local geological conditions, amount of slip and rupture lengths during the occurrence of each earthquakes, impact of human activities etc.

Appendix A

MATLAB code For Four-Cornered Chaos Game

```
close all; clear all; clc;
rng('default')

nvrtx = 4;
coarsegrain = xlsread('coarsegrain.xlsx');
vrtx = [0 0 ;16 0; 0 16 ;16 16];
size=size(coarsegrain);
iterations = size(1,1);

%%% For 1-bit Fractal Addresses %%%
bit = zeros(iterations,2) ;
bit(1,:)=vrtx(4,:)/2;

for i = 2:iterations
    vIdx = coarsegrain(i-1,1);
    bit(i,:) = vrtx(vIdx,:) - (vrtx(vIdx,:) - bit(i-1,:))/2;
end

figure,
cla
```

```
plot(bit(:,1),bit(:,2),'LineStyle','none','Marker','.','MarkerSize',5)

%%% For 4-bit Fractal Addresses %%%
fourbit= zeros(16,16);
k=1;
j=1;
for i=1:iterations
    for k=1:16
        if (bit(i,1)<=k && bit(i,1)>(k-1))
            for j=1:16
                if( bit(i,2)<=j && bit(i,2)>(j-1))
                    fourbit(k,j)=fourbit(k,j)+1;
                end
            end
        end
    end
end

s = sum(fourbit,'all');
figure,
pcolor(1:16,1:16,fourbit);
caxis([0 300]);


%%% For 8-bit Fractal Addresses %%%
vertexeit = [0 0 ;256 0; 0 256 ;256 256];
pnteit = zeros(iterations,2) ;
pnteit(1,:)=vertexeit(4,:)/2;

for i = 2:iterations
    vIdx = coarsegrain(i-1,1);
    pnteit(i,:) = vertexeit(vIdx,:)-(vertexeit(vIdx,:)-pnteit(i-1,:))/2;
end
```

```
eitbit= zeros(256,256);
k=1;
j=1;

for i=1:iterations
    for k=1:256
        if (pnteit(i,1)<=k && pnteit(i,1)>(k-1))
            for j=1:256
                if( pnteit(i,2)<=j && pnteit(i,2)>(j-1))
                    eitbit(k,j)=eitbit(k,j)+1;
                end
            end
        end
    end
end

s2 = sum(eitbit,'all');
figure,
pcolor(1:256,1:256,eitbit);
caxis ([0 5]);

figure,
subplot(2,2,1)
pcolor(1:256,1:256,eitbit);
axis([1 256 1 256])
caxis ([0 5]);

subplot(2,2,2)
pcolor(1:16,1:16,fourbit);
axis([1 16 1 16])
caxis([0 300]);
```

Appendix B

MATLAB code for Six-Cornered Chaos Game

```
close all; clear all; clc;
rng('default')

%% Defines number of vertices %%
nvertex = 6;

%% Defines the file name, stored in the same location, containing coarse
grain magnitudes, starting column-wise from first row %%
coarsegrain = xlsread('coarsegrain_usgs.xlsx');

%% Defines the vertices %%
vertex = [3 0 ; 9 0 ; 0 5.196 ; 12 5.196 ; 3 10.392 ; 9 10.392];

size=size(coarsegrain);

%% Specifies the number of iterations (= number of data points) %%
iterations = size(1,1);
bit = zeros(iterations,2);
bit(1,:)=vertex(4,:)/2;
```

```
%% Generate the points %%
for i = 2:iterations
    vIdx = coarsegrain(i-1,1);
    bit(i,:) = vertex(vIdx,:) - (vertex(vIdx,:) - bit(i-1,:))/2;
end

figure,
cla
plot(bit(:,1),bit(:,2),'LineStyle','none', 'Marker','.','MarkerSize',5)

hold on
```

Appendix C

Python code for determining the conditional probabilities

```
import io
import pandas as pd
from google.colab import files
values = pd.read_csv(Folder\_Path/File\_Name.csv')

initial_list=list()
for i in values['Coarse-Grain']:
    initial_list.append(i)

def split_sequence(sequence, n_steps):
    X, y = list(), list()
    for i in range(len(sequence)):
        # find the end of this pattern
    end_ix = i + n_steps
        # check if we are beyond the sequence
    if end_ix > len(sequence)-1:
        break
        # gather input and output parts of the pattern
    seq_x, seq_y = sequence[i:end_ix], sequence[end_ix]
    X.append(seq_x)
```

```
    y.append(seq_y)
return array(X), array(y)

from numpy import array
from keras.models import Sequential
from keras.layers import LSTM
from keras.layers import Dense

# split a univariate sequence into samples
def split_sequence(sequence, n_steps):
    X, y = list(), list()
    for i in range(len(sequence)):
        # find the end of this pattern
    end_ix = i + n_steps
        # check if we are beyond the sequence
    if end_ix > len(sequence)-1:
        break
    # gather input and output parts of the pattern
    seq_x, seq_y = sequence[i:end_ix], sequence[end_ix]
    X.append(seq_x)
    y.append(seq_y)
return array(X), array(y)

# define input sequence
raw_seq = initial_list
# choose a number of time steps
n_steps = 1
# split into samples
X, y = split_sequence(raw_seq, n_steps)
```

Bibliography

[1] Bilham, R., 2019. Himalayan earthquakes: a review of historical seismicity and early 21st century slip potential. Geological Society, London, Special Publications, 483, pp.SP483-16.

[2] Federal Emergency Management Agency, [Accessed: 10 May 2019] https://www.fema.gov/media-library-data/20130726-1504-20490-4864/fema_159_units.pdf

[3] G.J.H. McCall, "Reference Module in Earth Systems and Environmental Sciences", 2013 [Accessed: 11 May 2019] https://www.sciencedirect.com/topics/earth-and-planetary-sciences/earthquake

[4] J. Guckenheimer and P. Holmes, *Nonlinear Oscillations, Dynamical Systems, and Bifurcations of Vector Fields*, Springer-Verlag, New York, 1983.

[5] J. Wisdom, "Rotational Dynamics of Irregularly Shaped Natural Satellites," *The Astronomical Journal*, Vol.94, No.5, 1987 pp. 1350–1360.

[6] McCaffrey, R., 2009. The tectonic framework of the Sumatran subduction zone. Annual Review of Earth and Planetary Sciences, 37, pp.345-366.

[7] Paudyal, H., 2012. Himalayan Seismic Activity: A Concise Picture. Himalayan Physics, 3, pp.35-37.

[8] Sarah Friedl, Study.com [Accessed: 09 May 2019] https://study.com/academy/lesson/what-is-an-earthquake-definition-history.html

[9] Singh, S.C. and Moeremans, R., 2017. Anatomy of the Andaman–Nicobar subduction system from seismic reflection data. Geological Society, London, Memoirs, 47(1), pp.193-204.

[10] The United States Geological Survey, [Accessed: 22 April 2019]
https://earthquake.usgs.gov/earthquakes/search/

[11] University of Wisconsin, [Accessed: 13 May 2019]
http://pages.cs.wisc.edu/~rgreen/honors_thesis/chaos_IFS.html

[12] University of Wisconsin, [Accessed: 13 May 2019]
http://pages.cs.wisc.edu/~rgreen/honors_thesis/IFS.html